

# ORGANIC REACTION MECHANISMS

EDITOR  
M. G. MOLONEY



2020



## Organic Reaction Mechanisms • 2020





# Organic Reaction Mechanisms • 2020

An annual survey covering the literature dated  
January to December 2020

*Edited by*

*M. G. Moloney*  
University of Oxford  
England, UK

**WILEY**

This edition first published 2024  
© 2024 John Wiley & Sons Ltd

All rights reserved. No part of this publication may be reproduced, stored in a retrieval system, or transmitted, in any form or by any means, electronic, mechanical, photocopying, recording or otherwise, except as permitted by law. Advice on how to obtain permission to reuse material from this title is available at <http://www.wiley.com/go/permissions>.

The right of M. G. Moloney to be identified as the author of this editorial material in this work has been asserted in accordance with law.

#### Registered Offices

John Wiley & Sons, Inc., 111 River Street, Hoboken, NJ 07030, USA

John Wiley & Sons Ltd, The Atrium, Southern Gate, Chichester, West Sussex, PO19 8SQ, UK

For details of our global editorial offices, customer services, and more information about Wiley products visit us at <http://www.wiley.com>.

Wiley also publishes its books in a variety of electronic formats and by print-on-demand. Some content that appears in standard print versions of this book may not be available in other formats.

Trademarks: Wiley and the Wiley logo are trademarks or registered trademarks of John Wiley & Sons, Inc. and/or its affiliates in the United States and other countries and may not be used without written permission. All other trademarks are the property of their respective owners. John Wiley & Sons, Inc. is not associated with any product or vendor mentioned in this book.

#### Limit of Liability/Disclaimer of Warranty

In view of ongoing research, equipment modifications, changes in governmental regulations, and the constant flow of information relating to the use of experimental reagents, equipment, and devices, the reader is urged to review and evaluate the information provided in the package insert or instructions for each chemical, piece of equipment, reagent, or device for, among other things, any changes in the instructions or indication of usage and for added warnings and precautions. While the publisher and authors have used their best efforts in preparing this work, they make no representations or warranties with respect to the accuracy or completeness of the contents of this work and specifically disclaim all warranties, including without limitation any implied warranties of merchantability or fitness for a particular purpose. No warranty may be created or extended by sales representatives, written sales materials or promotional statements for this work. The fact that an organization, website, or product is referred to in this work as a citation and/or potential source of further information does not mean that the publisher and authors endorse the information or services the organization, website, or product may provide or recommendations it may make. This work is sold with the understanding that the publisher is not engaged in rendering professional services. The advice and strategies contained herein may not be suitable for your situation. You should consult with a specialist where appropriate. Further, readers should be aware that websites listed in this work may have changed or disappeared between when this work was written and when it is read. Neither the publisher nor authors shall be liable for any loss of profit or any other commercial damages, including but not limited to special, incidental, consequential, or other damages.

#### ***Library of Congress Cataloging-in-Publication Data Applied for:***

Hardback ISBN: 9781119716839

Set in 10/12pt WarnockPro by Straive, Chennai, India

## List of Contributors

- K. K. BANERJI** Formerly of Department of Chemistry, J. N. V. University, Jodhpur, India
- C. T. BEDFORD** Department of Chemistry, University College London, London, UK
- M. L. BIRSA** Faculty of Chemistry, "Al. I. Cuza" University of Iasi, Iasi, Romania
- I. BOSQUE** Instituto de Síntesis Orgánica and Departamento de Química Orgánica, Facultad de Ciencias, Universidad de Alicante, Alicante, Spain
- J. M. COXON** Department of Chemistry and Physics, University of Canterbury, Christchurch, New Zealand
- M. R. CRAMPTON** Department of Chemistry, University of Durham, Durham, UK
- N. DENNIS** Stretton, Queensland, Australia
- J. C. GONZALEZ-GOMEZ** Instituto de Síntesis Orgánica and Departamento de Química Orgánica, Facultad de Ciencias, Universidad de Alicante, Alicante, Spain
- P. KOČOVSKÝ** Department of Organic Chemistry, Charles University, Czech Republic
- and*
- Institute of Organic Chemistry and Biochemistry, Academy of Sciences of the Czech Republic, Czech Republic
- J. G. MOLONEY** Department of Chemistry, University of Oxford, Chemistry Research Laboratory, Mansfield Road, Oxford

**M. G. MOLONEY**

Department of Chemistry, University of Oxford,  
Chemistry Research Laboratory, Mansfield Road, Oxford

*and*

Oxford Suzhou Centre for Advanced Research, Jiangsu,  
P.R. China

**V. M. MOREIRA**

Laboratory of Pharmaceutical Chemistry, Faculty of  
Pharmacy, University of Coimbra, Portugal

*and*

Centre for Neuroscience and Cell Biology, University of  
Coimbra, Portugal

*and*

Centre for Innovative Biomedicine and Biotechnology,  
University of Coimbra, Portugal

**A. F. PARSONS**

Department of Chemistry, University of York,  
Heslington, York, UK

**T. F. PARSONS**

Wyke Sixth Form College, Hull, UK

**G. W. WEAVER**

Department of Chemistry, Loughborough University,  
Loughborough, Leicestershire, UK

## Preface

This volume, the 56th in the series, surveys research reporting organic reaction mechanisms described in the available literature dated 2020. That particular year is noteworthy for the arrival of the coronavirus pandemic, and of interest is that the global interruption to normal life appears to have had little impact on research productivity, possibly because lockdowns gave authors the opportunity to catch up with publication writing. The format of this volume follows directly on from that of ORM2019, although unfortunately the Carbenes and Nitrenes chapter has been omitted in the hard copy. It is expected that this chapter will be available in the online version in due course.

I acknowledge that this year marks the final contribution from Nick Dennis, and I offer sincere thanks for his long service and submission of high-quality chapters covering cycloadditions since 1989. I am also very pleased to welcome Syed Hussaini, who will now cover this chapter.

University of Oxford  
31 December 2023

M. G. Moloney



## Contents

- 1 Reactions of Aldehydes and Ketones and Their Derivatives** 1  
*M. G. Moloney*
- 2 Reactions of Carboxylic, Phosphoric, and Sulfonic Acids and Their Derivatives** 47  
*C. T. Bedford*
- 3 Oxidation and Reduction** 65  
*K. K. Banerji*
- 4a Nucleophilic Aromatic Substitution** 141  
*M. R. Crampton*
- 4b Electrophilic Aromatic Substitution** 179  
*G. W. Weaver*
- 5 Carbocations** 205  
*V. M. Moreira*
- 6 Nucleophilic Aliphatic Substitution 2020** 237  
*J. G. Moloney and M. G. Moloney*
- 7 Carbanions and Electrophilic Aliphatic Substitution** 267  
*M. L. Birsa*
- 8 Elimination Reactions** 281  
*M. L. Birsa*
- 9 Addition Reactions: Polar Addition** 295  
*P. Kočovský*
- 10 Addition Reactions: Cycloaddition** 401  
*N. Dennis*
- 11 Molecular Rearrangements** 433  
*J. M. Coxon*

**12 Ligand-Promoted Catalyzed Reactions** 507

*I. Bosque and J. C. Gonzalez-Gomez*

**13 Radical Reactions** 541

*A. F. Parsons and T. F. Parsons*

**Subject Index** 599



## 1

## Reactions of Aldehydes and Ketones and Their Derivatives

M. G. Moloney

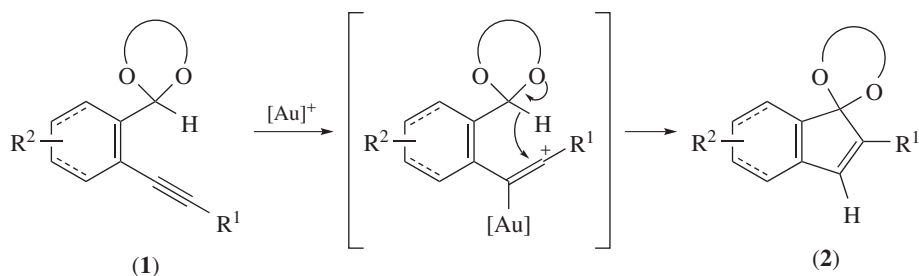
Department of Chemistry, University of Oxford, Chemistry Research Laboratory, Mansfield Road, Oxford  
Oxford Suzhou Centre for Advanced Research, Jiangsu, P.R. China

### CHAPTER MENU

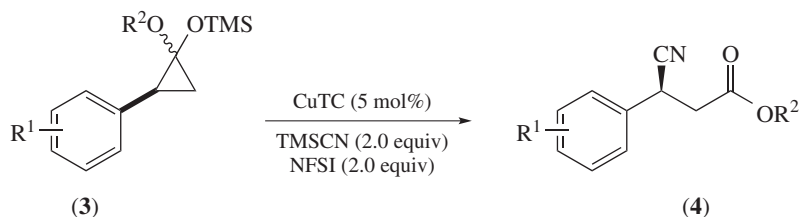
Formation and Reactions of Acetals and Related Species, 1
Reactions of Glucosides, 3
Reactions of Ketenes and Related Cumulenes, 6
Formation and Reactions of Nitrogen Derivatives, 9
Imines: Synthesis and General and Iminium Chemistry, 9
Mannich and Mannich-Type Reactions, 14
Stereoselective Hydrogenation of Imines, and Other Redox Processes, 15
Cyclizations of Imines, 15
Other Reactions of Imines, 15
Oximes, Oxime Ethers, and Oxime Esters, 18
Hydrazones and Related Species, 21
Iminium Ion Chemistry, 21
C—C Bond Formation and Fission: Aldol and Related Reactions, 26
The Asymmetric Aldol, 26
The Morita–Baylis–Hilman Reaction and Its Aza-Variants, 26
Other Aldol and Aldol-Type Reactions, 28
The Michael Addition, 29
The Wittig and Other Olefinations, 31
Miscellaneous Additions, 31
Reactions of Enolates and Related Reactions, 32
Oxidation of Carbonyl Compounds, 36
Reduction of Carbonyl Compounds, 36
Miscellaneous Reactions, 37
References, 37

### Formation and Reactions of Acetals and Related Species

The gold-catalyzed cyclization of 2-alkynylarylaldehyde cyclic acetals (**1**) leads to indenone derivatives (**2**) in good-to-excellent yields (Scheme 1). The cyclization occurs via a 1,5-H shift, favored by the cyclic acetal group, which both activates the benzylic C—H bond and prevents alkoxy migration.<sup>1</sup> A detailed study of the mechanism of this process has been investigated using density functional theory calculations. The reaction proceeds by initial coordination of Au(I) to the alkyne, which induces a 1,5-H shift (the rate-determining step), the rate of which depends on the electronic environment. Cyclization, 1,2-H shift, and then elimination lead to product formation; however, an aryl group on the alkyne is required for rapid reaction; otherwise, the cyclization becomes thermodynamically disfavored.<sup>2</sup>

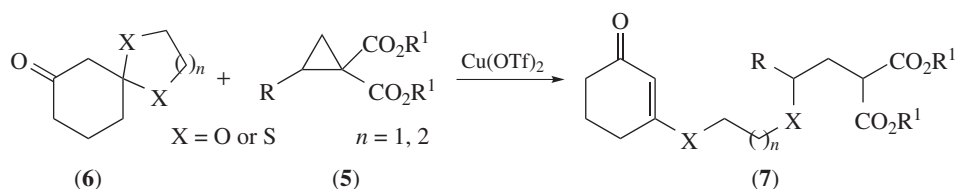


Scheme 1



Scheme 2

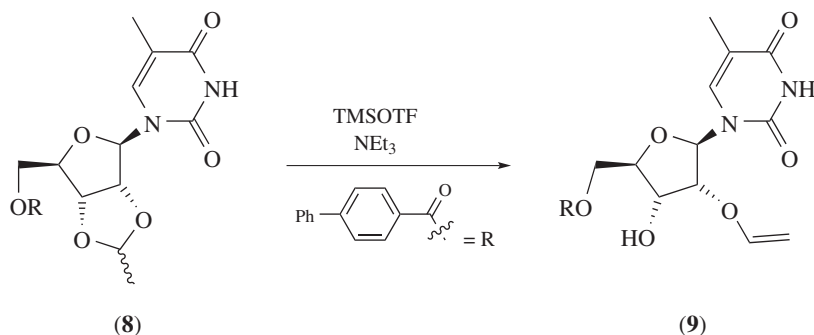
The cyanation of cyclopropanone acetals (**3**) giving  $\beta$ -carbonyl nitriles (**4**) with excellent enantioselectivity has been reported (Scheme 2). Mechanistically, a ring opening of an intermediate cyclopropanoxy radical leads to a benzylic radical, which is followed by cyanation.<sup>3</sup> (ee) The ring opening of donor–acceptor cyclopropanes (**5**) using 1,3-cyclohexanedione cyclic ketals and thioketals (**6**) as *O*- and *S*-nucleophiles, respectively, catalyzed by  $\text{Cu}(\text{OTf})_2$ , leads to alkylene glycol diethers and dithiol diethers (**7**) in good to high yields under mild conditions (Scheme 3).<sup>4</sup> The selective ring opening of a cyclic acetal (**8**) with  $\text{TMSOTf}$  and  $\text{NEt}_3$  leads to vinyl ether (**9**) and can be applied to the synthesis of highly functionalized nucleoside vinyl ethers (Scheme 4).<sup>5</sup>



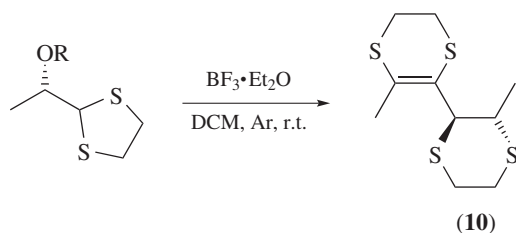
Scheme 3

Chiral 2,3-dihydro-1,4-dithiine derivatives (**10**) are available by the reaction of chiral cyclic hydroxy dithioacetals in the presence of boron trifluoride diethyl etherate (Scheme 5), in a mechanism involving internal nucleophilic  $\text{S}_{\text{N}}2$  substitution of the hydroxyl group by sulfur and then formation of a bicyclic thiiranium cation, ring expansion, and dimerization.<sup>6</sup>

Tandem Prins cyclizations for the construction of fused scaffolds have been reviewed.<sup>7</sup> A review describes Pd-catalyzed anti-Markovnikov oxidations of aromatic and aliphatic terminal alkenes to give terminal acetals (oxidative acetalization) and aldehydes (Wacker-type oxidation). Importantly, the addition of electron-deficient cyclic alkenes such as *p*-benzoquinones and maleimides facilitates nucleophilic attack of oxygen nucleophiles on coordinated terminal alkenes and also serves to oxidize Pd(0) depending on the reaction



Scheme 4



Scheme 5

conditions. The steric demand of nucleophiles, slow substrate addition, and halogen-directing groups are also key parameters.<sup>8</sup>

## Reactions of Glucosides

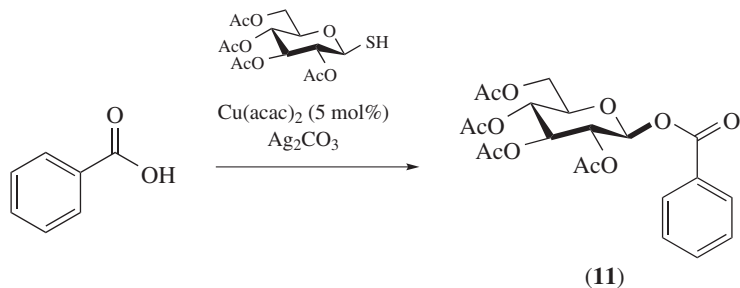
Hydrogen bonding in carbohydrate systems has been of interest. Vacuum ultraviolet (VUV) electronic circular dichroism (ECD) spectra of D-glucose,  $\alpha$ -D-glucopyranose, and  $\beta$ -D-glucopyranose were measured in aqueous solution down to 163 nm using a synchrotron radiation VUV-ECD spectrophotometer. Theoretically calculated spectra (using molecular dynamics (MD) simulations with explicit water molecules and time-dependent density functional theory (TDDFT)) reproduced the experimentally observed spectra and confirmed that VUV-ECD distinguished the  $\alpha$ -anomer and  $\beta$ -anomers and the three gauche (G) and trans (T) rotamer conformations (GT, GG, and TG) of the hydroxymethyl group at C-5. This was possible from changes in the degree of hydration of intramolecular hydrogen bonds around the hydroxymethyl group and the hydroxyl group at C-1.<sup>9</sup> Using *ab initio* MD simulations, it has been shown that for three D-glucose isomers ( $\alpha$ ,  $\beta$ , and open chain) in 1-ethyl-3-methylimidazolium acetate solution in the presence and absence of water, every hydrogen bond elongates, except the glucose–glucose hydrogen bond for the open chain and the  $\alpha$ -form, which both shorten, indicating the beginning of crystallization. The glucose ring rearranges from on-top to in-plane, and the open form changes from a coiled to a more linear arrangement.<sup>10</sup> The hydration of glucosamine has been studied by Car-Parrinello MD, which shows that the hydroxyl groups form stable hydrogen bonds with the water molecules with intensities ranging from weak (closed-shell interaction) to intermediate (partially covalent interactions). The main contribution to stabilizing energies comes from  $n \rightarrow \sigma^*$  hyperconjugation, and the energy barrier for the proton transfer from water to the amino group is  $0.88 \text{ kcal mol}^{-1}$ . This low protonation energy barrier shows that glucosamine can be

protonated in an aqueous environment at room temperature.<sup>11</sup> Using cellulose (an infinitely repeating polymer of D-glucose) as an example, MD modeling has been used to show that the thermal excitation of intermolecular stretching modes leads to lengthening and weakening of intermolecular O—H ··· O hydrogen bonds, indirectly strengthening the associated covalent O—H bonds; this is responsible for temperature-dependent blue shifting of O—H stretching bands in the IR spectra of carbohydrate biopolymers.<sup>12</sup>

DFT calculations have been used to understand anomerizations and mutarotation equilibria and, importantly, show the role not only of the aldehyde intermediate but also its hydrated form, which is often more abundant in the equilibrium. Moreover, different mutarotation mechanisms may operate for every monosaccharide, and pyranose–furanose interconversion may actually occur without the intermediacy of open-chain forms. For D-glucose, D-ribose, and D-xylose, all structures involved in mutarotation undergo interconversion pathways, whose energy barriers calculated at the M06-2X/6-311++G(d,p) level are in good agreement with previous experimental measurements.<sup>13</sup>

Glycosylation reactions in a series of bicyclic C-2-substituted pyranoside models are best understood by the bent bond/antiperiplanar hypothesis orbital model, which invokes hyperconjugation interactions between groups at C-2 and the two  $\tau$  bonds (bent bonds) of oxocarbenium ion intermediates formed under the glycosylation conditions. Thus, nucleophiles add to oxocarbenium intermediates by  $S_N2$ -like antiperiplanar displacement of the weaker of the two  $\tau$  bonds.<sup>14</sup> The activation of both “armed” and “disarmed” type glycols toward direct glycosylation may be controlled by the choice of oxidation state and counterion of a copper catalyst; the process gives deoxyglycosides in good to excellent yields. Mechanistic studies show that CuI is essential for effective catalysis and stereocontrol and that the reaction proceeds through dual activation of both the enol ether and the hydroxyl nucleophile.<sup>15</sup> A review covering the chemoenzymatic production of fluorinated carbohydrates, focusing on activated fluorinated donors and enzymatic glycosylation involving fluorinated sugars as either glycosyl donors or acceptors, has appeared.<sup>16</sup> The trifluoromethylation of glycols using  $CF_3SO_2Na$  as the trifluoromethyl source and  $MnBr_2$  as the redox mediator under electrochemical conditions in 60–90% yields with high regioselectivity has been reported. The reaction proceeds by a radical mechanism.<sup>17</sup> A note that the use of the term electron-donating benzyl groups is misguided has appeared and that benzyl ethers (OBn) should more correctly be referred to as inductively electron withdrawing, even if they are less so than benzoyl esters (OBz).<sup>18</sup>

The reaction of 1-thiosugars with carboxylates in the presence of a catalytic amount of  $Cu(acac)_2$  or  $Co(acac)_2$  and  $Ag_2CO_3$  as an oxidant in  $\alpha,\alpha,\alpha$ -trifluorotoluene gives substituted O-glycoside esters (**11**) in good to excellent yields with 1,2-*trans*-selectivity (Scheme 6). The reaction mechanism, established by cyclic voltammetry, proceeds by oxidation of the thiosugar to give the corresponding disulfide; complexation with silver(I) leads to the formation of the acetoxonium ion, which is trapped by the carboxylate to give the product.<sup>19</sup> Detailed kinetic



Scheme 6

models of transacylation and hydrolysis reactions for phenylacetic acid acyl glucuronides and their analogous acyl glucosides have been developed. The transacylation reaction was modeled using DFT, and the calculated activation energy showed a close correlation with the degradation rate of the 1- $\beta$  anomer.<sup>20</sup>

Tandem mass spectrometry under positive ionization mode may be used to distinguish isomeric Schiff bases and Amadori products,<sup>21</sup> and MS/MS fragmentation patterns under negative ionization mode have been used to study Maillard reaction mixtures.<sup>22</sup> The major diagnostic ion of the Schiff base was found to be a diose attached to the amino acid residue, while that of the Amadori compound was a triose. The ball milling of glucose with different amino acids almost exclusively results in the formation of a mixture of Schiff bases and Amadori compounds, and amino acids with basic side chains generated more Schiff bases and those with acidic side chains generated more Amadori products.

The isomerization of glucose to fructose over a 1-butanol/hydrotalcite catalytic system gives fructose in 50% yield with selectivity exceeding 80% at a glucose concentration of 10 wt%; under these conditions, the leaching of  $\text{Mg}^{2+}$  from hydrotalcite is negligible, and the reactions appear to proceed by the base-catalyzed deprotonation of the C-2 position in glucose.<sup>23</sup> The mechanisms for the conversion of  $\beta$ -xylopyranose and methanol to methyl lactate, glycolaldehyde, and water over zirconia surfaces have been reported, and involve aldose–ketose or ketose–aldose tautomerization and retro–aldol condensation reactions. The rate-determining step is the ketose–aldose tautomerization of deprotonated glycerosone to deprotonated glyceraldehyde. For the retro–aldol condensation reaction, the rate-determining step is associated with C3–H bond formation, which relies on the ability of the  $\text{H}_2\text{O}$  ligand to provide the proton.<sup>24</sup> Glycosidic bond activation in cellulose pyrolysis has been studied by density functional theory calculations of the model compound, maltose, and shows that the intramolecular C-2 hydroxyl group favorably interacts with lone pairs on the ether oxygen of an  $\alpha$ -glycosidic bond. This process has an activation energy of  $219 \text{ kJ mol}^{-1}$ , which is similar to that of noncatalytic transglycosylation ( $209 \text{ kJ mol}^{-1}$ ). The results help explain the lack of sensitivity of depolymerization kinetics to glycosidic bond stereochemistry. Constrained *ab initio* MD simulations show that vicinal hydroxyl groups in a reacting carbohydrate melt anchor transition states via two-to-three hydrogen bonds and lead to lower free energy barriers (similar to  $134\text{--}155 \text{ kJ mol}^{-1}$ ).<sup>25</sup> The mechanism of the conversion of  $\beta$ -cellobiose to 5-hydroxymethylfurfural (HMF) catalyzed by a Brønsted acid ( $\text{H}_3\text{O}^+$ ) in aqueous solution has been studied using quantum chemical calculations at the M06-2X/6-311++G(d,p) level under a polarized continuum model (PCM-SMD). Three reaction pathways have been identified, involving cellobiulose and glycosyl-5-hydroxymethylfurfural (the thermodynamically predominant pathway), through cellobiulose and fructose, and through cellobiulose and glucose (kinetically dominant pathway), for which the rate-determining steps are associated with the intramolecular [1,2]-H shift in the aldose–ketose tautomerization. Halide anions ( $\text{Cl}^-$  and  $\text{Br}^-$ ) act as promoters, while both nitrate and carboxylate behave as inhibitors. The roles of these anions in  $\beta$ -cellobiose conversion to 5-hydroxymethylfurfural can be correlated with their electrostatic potential and atomic number, which may cause a decrease in the relative enthalpy energy and the value of entropy when interacting with the cation.<sup>26</sup>

The synthesis of the bicyclic sugar bradyrhizose in 14 steps and a 6% overall yield from D-glucose have been reported.<sup>27</sup> *N*-Substituted derivatives of 1,4-dideoxy-1,4-imino-D-mannitol, the pyrrolidine core of swainsonine, have been synthesized efficiently and stereoselectively from D-mannose; *N*-alkylated, *N*-alkenylated, *N*-hydroxyalkylated, and *N*-aralkylated derivatives are all available. *N*-Substitution was found to decrease  $\alpha$ -mannosidase inhibitory activities, but some showed significant inhibition of other glycosidases.<sup>28</sup> D-Allose, the C-3 epimer of D-glucose, is a naturally occurring rare monosaccharide, and the synthesis of D-allose-6-phosphate derivatives with biodegradable protecting groups for the study of

cytotoxic activity has been reported.<sup>29</sup> Fluorine-18-labeled nitroso derivatives of streptozotocin have been prepared for use as glycoside analogs for *in vivo* GLUT2 imaging; these were found to accumulate in GLUT2-expressing organs (liver and kidney) within 5 min of administration.<sup>30</sup> Cyclohexenyl-based carbasugars of  $\alpha$ -D-glucopyranoside have been prepared and shown to be good covalent inhibitors of a glycoside hydrolase, with better-leaving groups reacting by an  $S_N1$  mechanism, while those for worse-leaving groups are limited by a conformational change of the Michaelis complex prior to a rapid  $S_N2$  reaction with the enzymatic nucleophile. Bicyclo[4.1.0]heptyl-based carbaglucooses react by pseudoglycosidic bond cleavage via an  $S_N1$  process in which the leaving group binds to the enzyme. In this process, the mechanism is obscured by conformational changes that the Michaelis complex of the enzyme and natural substrate make before the attack of the nucleophile.<sup>31</sup> C-Glycosidically-linked phospholipid derivatives of 4-amino-4-deoxy-L-arabinose have been prepared as hydrolytically stable and chain-shortened mimics of the native undecaprenyl analog.<sup>32</sup>

A combined experimental and computational mechanistic study of pyranylation and 2-deoxygalactosylation catalyzed by a cationic thiourea organocatalyst has identified two distinct reaction pathways involving either dual hydrogen bond (H-bond) activation or Brønsted acid catalysis. The former proceeded in an asynchronous concerted manner, but the latter led to the formation of an oxocarbenium intermediate accompanied by subsequent alcohol addition.<sup>33</sup>

The deprotonation of differently substituted propargyl xylosides with *s*-BuLi/TMEDA followed by protonation with *t*-butanol provided a range of new axially chiral 1,3-disubstituted alkoxyallenes. DFT calculations on the propargyl/allenyl lithium intermediates indicated the importance of the approach of the alcohol toward the lithium compounds in the reaction product.<sup>34</sup>

The  $\beta$ -glycosidase activity at neutral and acidic pH of 4'-substituted flavonols glycosylated with D-glucose, *N*-acetyl-D-glucosamine, and D-glucuronic acid has been found to be fastest in an acidic environment that accelerated enzymatic hydrolysis for 4'-chloroflavonyl glycosides, while 4'-dimethylaminoflavonyl glucoside is not reactive at all. Thus, the rate of enzymatic hydrolysis increases as the electron-withdrawing nature of the 4'-substituent increases.<sup>35</sup>

Hydroxylamines and weakly basic amines may be used as nucleophiles in the oxidative deamination of *N*-nitroso *N*-acetylneuraminic acid (NeuAc) derivatives leading to 5-desamino-5-hydroxy NeuAc; the  $pK_a$  of the nucleophile determines product formation, with more acidic species affording only substitution at the 5-position, while less acidic species give mixtures of elimination products and disubstitution products.<sup>36</sup>

## Reactions of Ketenes and Related Cumulenes

Microsecond pulsed infrared laser decomposition of thin 1,3,5-trinitro-1,3,5-triazinane ((O<sub>2</sub>NNCH<sub>2</sub>)<sub>3</sub>, RDX) films at 5 K led to the detection of a product signal at  $m/z = 42$  due to ketene (H<sub>2</sub>CCO), but not to diazomethane (H<sub>2</sub>CNN) as has been previously suggested.<sup>37</sup> The rate constants at 298 K of the reactions HCCO + O<sub>2</sub> and HCCCO + O<sub>2</sub> have been shown to be  $k = (6.3 \pm 1.0) \times 10^{-13}$  and  $(5.7 \pm 0.6) \times 10^{-12}$  cm<sup>3</sup> mol<sup>-1</sup> s<sup>-1</sup>, respectively.<sup>38</sup>

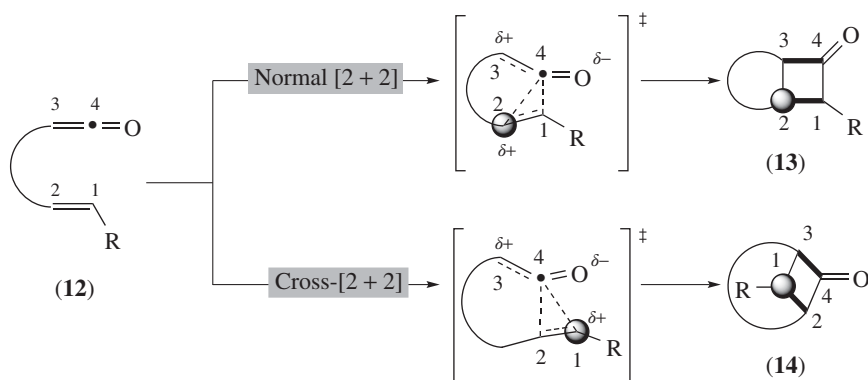
The H-abstraction reaction from the methyl group of acetamide CH<sub>3</sub>CONH<sub>2</sub> to produce the 2-amino-2-oxoethyl radical ( $\bullet$ CH<sub>2</sub>CONH<sub>2</sub>) was the sole reaction in a *para*-hydrogen quantum-solid matrix host at 3.3 K, consistent with theoretical predictions that this reaction has the smallest barrier; this reactivity mode is important for astrochemical reaction modeling. The amide bond of acetamide is unaffected. The photolysis of ( $\bullet$ CH<sub>2</sub>CONH<sub>2</sub>) at wavelengths 380–450 nm produces ketene.<sup>39</sup>

That the acetyl peroxy radical ( $\bullet\text{O}_2\text{C(O)Me}$ ) is a precursor in the formation of tropospheric ketene has been shown using high-level quantum chemical calculations (Scheme 7); its nitration is also known to lead to the formation of peroxy acetyl nitrate. The dissociation of acetylperoxy radicals into ketene and hydroperoxy radicals occurs most likely by excitation, which is red-light driven to give ketene $\cdot\text{HO}_2$ , ketene $\cdot\text{H}_2\text{O}\cdot\text{HO}_2$ , and ketene $\cdot(\text{H}_2\text{O})_2\cdot\text{HO}_2$ . These product complexes possess a long lifetime, but their atmospheric abundances decrease with increasing altitudes.<sup>40</sup>



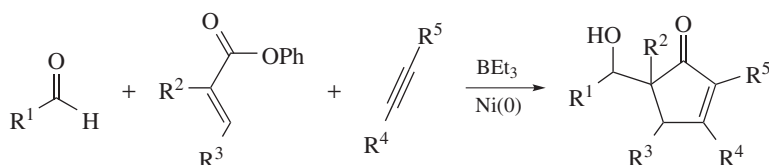
Scheme 7

A DFT study on the mechanism and regioselectivity of intramolecular [2 + 2] cycloadditions of ene-ketenes (**12**), leading to either fused-ring (**13**) (via normal [2 + 2] cycloaddition) or bridged-ring (**14**) (via cross-[2 + 2] cycloaddition) cyclobutanones, indicates that these [2 + 2] cycloadditions are concerted (Scheme 8). The normal [2 + 2] cycloaddition transition state forms an internal carbocation, while the cross-[2 + 2] cycloaddition transition state generates an external carbocation; consideration of the relative stability of these carbocations allows prediction of the regiochemistry.<sup>41</sup>



Scheme 8

The three-component cycloaddition of enoates, alkynes, and aldehydes proceeds by a [3 + 2] cycloaddition and alkylation leading to cyclopentenones, catalyzed by Ni(0) and  $\text{Et}_3\text{B}$  (Scheme 9). Computational investigation identified three energetically feasible mechanistic pathways, the most likely of which proceeds by initial ketene formation, followed by carbocyclization and aldol reaction. However, the formation of a seven-membered metallacycle intermediate becomes possible when an  $\alpha$ -substituted enoate is used; this appears to be due to more difficult phenoxide elimination leading to ketene formation.<sup>42</sup>



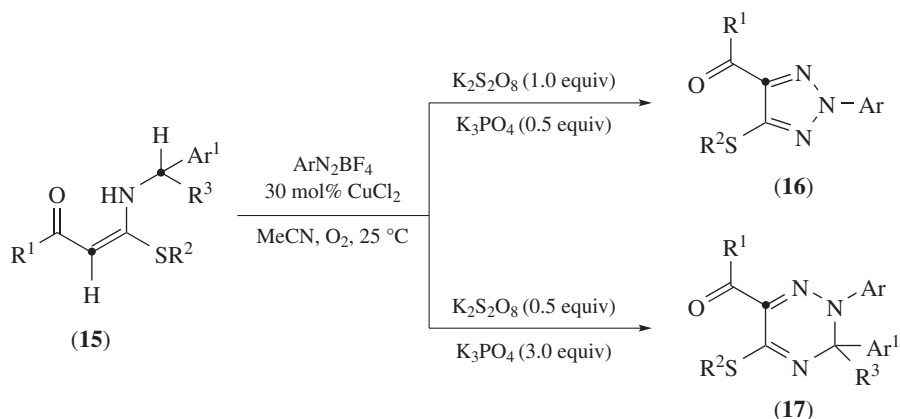
Scheme 9

Catalytic hydrogenolysis of the *Z*-isomer of an aryl-substituted ketene  $\beta$ -lactones gave deoxypropionate derivatives favoring the *anti*-diastereomer and with excellent enantioselectivity (up to 99% *ee*). A nonlinear relationship between diastereoselectivity and aryl substituent  $\sigma$  values was found. The reactions appear to proceed by *anti*- $\beta$ -elimination and an *anti*-selective hydrogenation of an *E*-isomer olefin intermediate.<sup>43</sup> The photoionization of fulvenone ( $c\text{-C}_5\text{H}_4=\text{C}=\text{O}$ ), a reactive ketene species relevant in the catalytic pyrolysis of lignin generated by the pyrolysis of 2-methoxy acetophenone, has been shown to have an adiabatic ionization energy of  $8.25 \pm 0.01$  eV.<sup>44</sup>

The catalytic methoxycarbonylation of ethene with a bidentate tertiary phosphine (DTBPX) and palladium has been studied by density functional theory (B3PW91-D3/PCM level). Of three different pathways for the formation of methyl propanoate, namely carbomethoxy, ketene, and hydride-hydroxyalkylpalladium pathways, the latter was found to be favored kinetically. After intermolecular methanolysis, a hydroxyalkylpalladium is formed.<sup>45</sup>

(4 + 2) and (2 + 2) Cycloadditions of keteniminium cations with 1,3-dienes have been studied computationally with B97X-D density functional theory. Reactions of keteniminium cations with 1,3-dienes are influenced by the *s-cis* or *s-trans* nature of the diene, the former giving an intermediate enamine that leads to the formation of (2 + 2) cycloadducts across the keteniminium C—C bond. The first step of the cycloaddition is rate-determining, and the reaction occurs by attack on the central carbon of the keteniminium cation and subsequent C—C bond formation. By contrast, *s-cis* dienes lead to preferential formation of (4 + 2) products by both stepwise and concerted mechanisms involving regioselective addition to the keteniminium C—N bond. Diels–Alder reaction occurs via a concerted mechanism if the diene termini are held in close proximity, as in cyclopentadiene.<sup>46</sup>

Ketene *N,S*-acetals (**15**) react with aryldiazonium salts using copper(II) catalysis to give 1,2,3-triazoles (**16**) and 2,3-dihydro-1,2,4-triazines (**17**), depending on the oxidant and base. The reaction proceeds via an alkenyl azo/imino hydrazone intermediate.<sup>47</sup>



The chemistry of ketene dithioacetals has been reviewed covering nucleophilic enethiols; formation of CPd-SR intermediates; C—S bond cleavage; substitution of SR; and reactions of the double bond.<sup>48</sup> The reaction of  $\alpha$ -substituted indolylmethyl methanols or  $\alpha$ -indolyl- $\alpha$ -amino carbonyl electrophiles and ketene dithioacetals under Brønsted-acid conditions provides diastereoselective access to 2,3-disubstituted cyclopenta[*b*]indoles by a formal [3 + 2] cycloaddition.<sup>49</sup>

Acetic acid decarboxylation and decarbonylation over a Pd(111) surface proceeds, for the former, through deprotonation of CH<sub>3</sub>COOH to acetate (CH<sub>3</sub>COO<sup>-</sup>), followed by conversion to carboxylmethylidene (CH<sub>2</sub>=C=O=O), C—H bond cleavage to carboxylmethylidyne



(CHCOO), and finally C—C bond cleavage to form CH and CO<sub>2</sub>. The latter decarbonylation pathway proceeds via the same initial dehydrogenation steps to CH<sub>2</sub>COO, followed by deoxygenation to ketene (CH<sub>2</sub>=C=O), dehydrogenation to ketyne (CHCO), and finally C—C bond cleavage to yield CH and C=O. Carboxylmethylidene (CH<sub>2</sub>COO), which is formed in both mechanisms, is a key reaction intermediate determining the bifurcation between decarboxylation and decarbonylation, for which the latter is favored.<sup>50</sup>

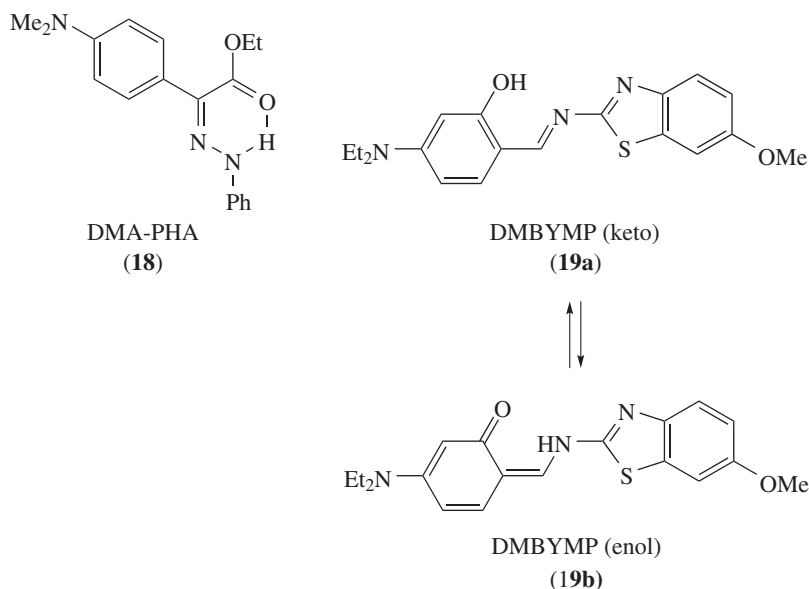
## Formation and Reactions of Nitrogen Derivatives

Lewis base amine/imine-mediated reactions,<sup>51</sup> and the chemistry of 1,3,5-trisubstituted 1,3,5-triazinanes (hexahydro-1,3,5-triazines), surrogates for formaldimines, have been reviewed.<sup>52</sup> A review of methodology to construct the common spirocyclic imine components of cyclic imine toxins has appeared; a particular focus is the use of  $\alpha,\beta$ -unsaturated *N*-acyl iminium ion dienophiles in Diels–Alder reactions, and of hydroamination of amino alkynes, which generate spirocyclic imines directly.<sup>53</sup> The application of directing groups to control site selectivity in transition-metal-catalyzed C–H functionalization reactions has been reviewed.<sup>54</sup>

## Imines: Synthesis and General and Iminium Chemistry

Something of the history of imines, and of Hugo Schiff himself, has been reviewed.<sup>55</sup> The kinetics of the condensation of *n*-butylamine and benzaldehyde have been studied by DFT calculations and microkinetic simulations.<sup>56</sup> The condensation of a primary aniline and 2-hydroxycyclobutanone promoted by a Brønsted acid gives tryptamine derivatives in moderate to good yields; a mechanism involving an  $\alpha$ -iminol rearrangement, ring expansion, ring closure, and a depart-and-return rearrangement process was proposed.<sup>57</sup> The conversion of *ortho*-aminobenzaldehydes to their corresponding imines in acetonitrile was investigated, and it was found that the acidity of OH/NH and the existence of H bonds influenced both the thermodynamics and kinetics of imine formation.<sup>58</sup> Vinylogous imines may be prepared from anilines and cinnamaldehydes, which react further in superacidic media to form quinolines.<sup>59</sup> A three-component reaction that proceeds by C–C and C–O bifunctionalization of olefins using molecular iodine and visible light leading to  $\gamma$ -iminolactones has been reported, but without metal catalysis. Iodine radicals generated under visible-light irradiation reacted with alkenes to form a highly reactive intermediate, which initiated the coupling of diiodide, malonate, and amine to give the iminolactone.<sup>60</sup>

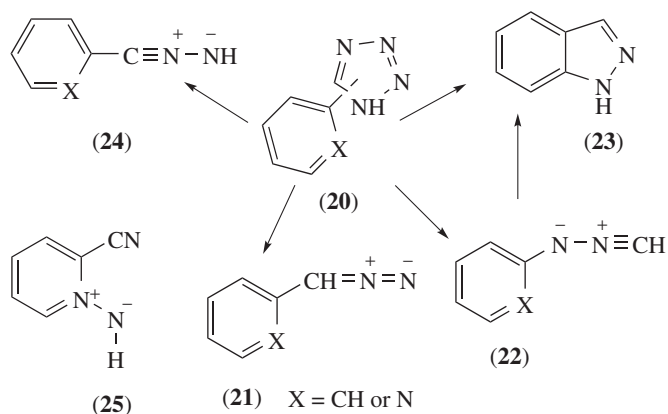
The photodynamics of switchable photoisomerization processes of a camphorquinone imine and alkene imine have been studied by trajectory surface-hopping (TSH) MD at the SA4-CASSCF/def2-SVP level.<sup>61</sup> The emission and switching mechanisms of a model photochromic phenylhydrazone have been studied using TD-DFT and CASPT2 calculations. The fluorescence-emitting *Z* configuration of DMA-PHA (**18**) does not involve an excited-state intramolecular proton transfer process, and the light-induced fluorescence toggling results from *E*  $\leftrightarrow$  *Z* interconversion driven by an out-of-plane C=N bond torsion assisted by a N–N single bond rotation, which leads to loss of fluorescence activity. Moreover, the N–N bond rotation reduces the photoisomerization yields.<sup>62</sup> The excited-state luminescent properties and intramolecular proton transfer of 5-(diethylamino)-2-(((6-methoxybenzo[*d*]thiazol-2-yl)imino)methyl)phenol (DMBYMP, **19a**, **b**) have been studied by DFT and TDDFT methods. An intramolecular hydrogen bond of DMBYMP becomes enhanced, facilitating keto/enol equilibration, and an intramolecular charge transfer initiates the proton transfer reaction.<sup>63</sup>



The flavin semiquinone intermediate found in flavoproteins has been generated by single electron reduction of the natural FMN cofactor using sodium ascorbate and has been characterized by UV–visible, fluorescence, and EPR spectroscopy.<sup>64</sup>

A mechanism for supercritical water oxidation of methylamine,  $\text{CH}_3\text{NH}_2$ , involving peroxy radical reaction, leading to imine formation, involves oxidation of the  $\bullet\text{CH}_2\text{NH}_2$  radical to methanimine,  $\text{CH}_2=\text{NH}$ , with subsequent hydrolysis giving ammonia and formaldehyde.<sup>65</sup> The oxidative coupling of primary alcohols and aromatic and aliphatic primary amines using 2 mol% polyoxometalate  $\text{Na-12}[\text{WZn}_3(\text{H}_2\text{O})_2(\text{ZnW}_9\text{O}_{34})_2]$  ( $\text{Zn-WZn}_3$ ) as a catalyst in the presence of *t*BuOK and di-oxygen leads to the formation of imines with up to 100% conversion and selectivity. The formation of a di-oxygen  $\text{Zn-WZn}_3$  activated species was proposed.<sup>66</sup>

Density functional theory and CASPT2 level calculations of the photolysis and flash vacuum pyrolysis (FVP) of tetrazoles (20) (Scheme 10) show that this is a convenient source of aryl diazo compounds (21) and their derived arylcarbenes. The conversion of *N*-phenylnitrile imine (22,  $\text{X} = \text{CH}$ ) to indazole (23) is favored, but the cyclization of *C*-phenylnitrile imine (24,  $\text{X} = \text{CH}$ ),

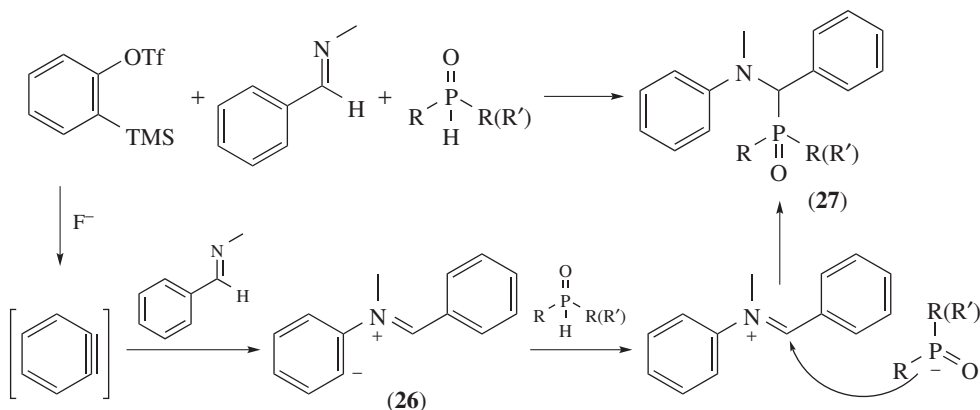


Scheme 10

which passes through a carbenic nitrile imine, requires a much higher activation energy and is therefore not competitive. *C*-(2-Pyridyl)nitrile imine (**24**, X = N) is predicted to undergo rearrangement to cyanopyridine *N*-imide (**25**), with an activation energy of 43 kcal mol<sup>-1</sup>. The experimental observation that 2-pyridyldiazomethane (**21**, X = N) is actually formed requires a reaction with a lower energy barrier, and this may be achieved by H-transfer from the tetrazole ring in 5-(2-pyridyl)tetrazole to the pyridine ring with subsequent formation of 1*H*-2-(diazomethylene)pyridine and elimination of N<sub>2</sub>.<sup>67</sup>

A theoretical investigation of the mechanism in the InCl<sub>3</sub>-catalyzed cycloaddition of *N*-tosyl formaldimine with alkenes or allenes has been conducted, suggesting that InCl<sub>2</sub><sup>+</sup> coordinated by dichloroethane (InCl<sub>2</sub><sup>+</sup>-DCE) is the plausible catalytic species generated *in situ*. The catalytic cycle then starts from the coordination of *N*-tosyl formaldimine to InCl<sub>2</sub><sup>+</sup>-DCE, to give an In-complexed iminium intermediate, which undergoes intermolecular *aza*-Prins reaction with the alkene substrate to form a carbocation intermediate. This is attacked by the second *N*-tosyl formaldimine molecule chemoselectively to give a formaldiminium intermediate. This intermediate then undergoes ring closure, leading to hexahydropyrimidine along with the regeneration of the catalyst. DFT results also indicate that *N*-tosyl-formaldimine also accelerates the 1,3-H-shift as a proton acceptor, giving an experimentally observed allylamide product.<sup>68</sup>

Aldimines, prepared from aldehydes and 2-aminobenzyl alcohols, may be cyclized by NHC-catalysis via the imidoyl azolium species, to trifluoromethylated 3,1-benzoxazines in good yields and broad scope.<sup>69</sup> 2-Substituted bithiazolidines, of relevance as penicillin analogs with inhibitory activity against metallo- $\beta$ -lactamases, have been prepared by aldehyde exchange with yields ranging from 31% to 75%; the reaction proceeds by *in situ* formation of imines. A previously proposed imine metathesis was found not to be plausible.<sup>70</sup>  $\alpha$ -Aminophosphonates are available in moderate to good yields by the reaction of imines with an *in situ* generated aryne in the presence of a dialkyl phosphite (Scheme 11); a mechanism involving nucleophilic addition of the imine to the aryne leads to an iminium zwitterion (**26**), which abstracts a proton from the dialkyl phosphite, to give a phosphite anion, which in turn adds to the iminium carbon, giving the  $\alpha$ -aminophosphonate product (**27**).<sup>71</sup>

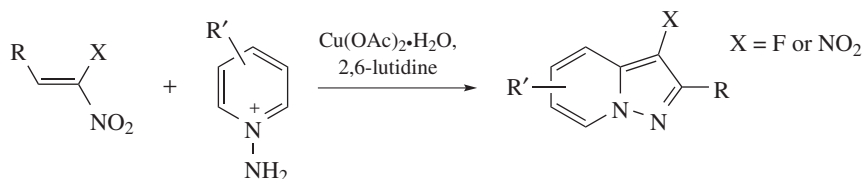


Scheme 11

The scandium(III) triflate-catalyzed synthesis of *N*-unprotected ketimines from the corresponding ketones in high yields with broad functional group tolerance has been reported.<sup>72</sup>

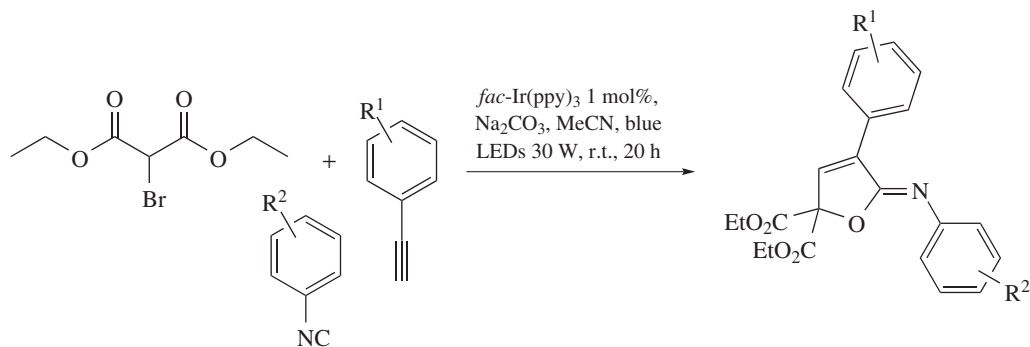
A multicomponent annulation of aryl thiocarbamates, internal alkynes, and sulfonamides leading to iminocoumarins proceeds with Rh-catalyzed and sulfur-directed C—H bond

activation. A mechanism involving nucleophilic attack of the sulfonamide on an intermediate iminium cation is a key step.<sup>73</sup> The annulation of substituted and unsubstituted nitroalkenes with *in situ* generated pyridinium imines leading to pyrazolo[1,5-*a*]pyridines by Cu(OAc)<sub>2</sub>-promoted oxidative catalysis has been reported (Scheme 12). The reaction tolerates electron-rich and electron-deficient nitroalkenes as well as different aminopyridinium salts, and a stepwise mechanism rather than a concerted [3 + 2]-mechanism is proposed.<sup>74</sup>



Scheme 12

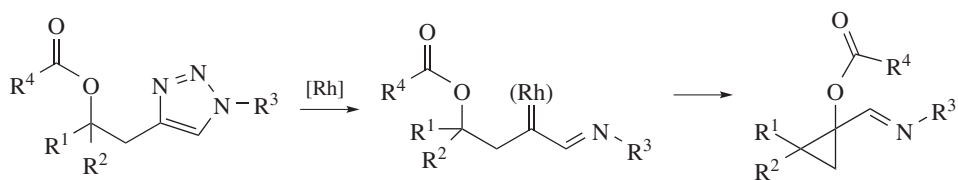
*N*-Arylated sulfoximines are accessible in high yield from 8-aminoquinoline-derived benzamides and sulfoximines by copper-catalyzed cross-dehydrogenative C–H/N–H coupling, in which C–H bond cleavage is the kinetically controlling step.<sup>75</sup> The synthesis of nonsymmetric iminophosphonamines Ph<sub>2</sub>P(NHR)(NR') (R = Me, *t*-Bu, *o*-Tol; R' = *p*-Tol, *o*-Tol, 2,6-Xyl, 2,6-Diip, *p*-Ts) by Kirsanov condensation, involving a double amination of a trihalophosphorane, which permits the introduction of at least one sterically bulky *N*-substituent, has been reported. The second amination step is shown to be highly sensitive to the steric bulk of the amine and the acidity of the aminohalophosphonium intermediate.<sup>76</sup> A photocatalyzed iridium-promoted three-component synthesis of iminofurans from an arylisocyanide, a bromomalonate, and an alkyne has been reported (Scheme 13).<sup>77</sup>



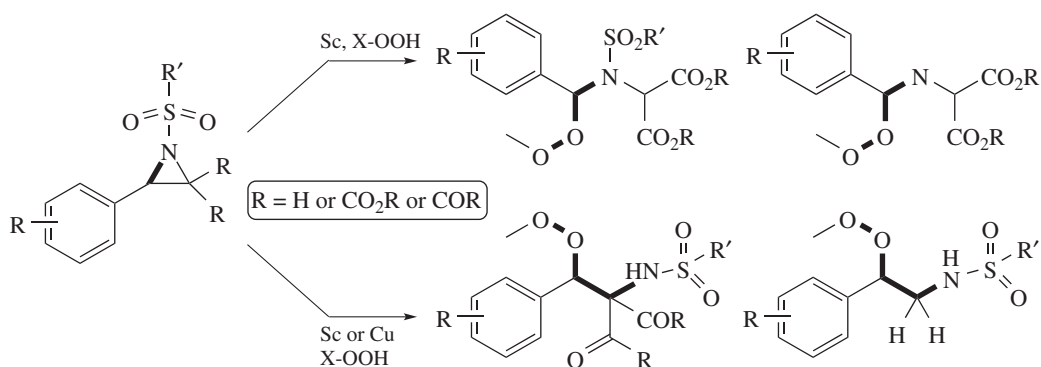
Scheme 13

$\alpha$ -Iminorhodium carbenes have been shown to mediate 1,3-migration of acyloxy groups leading to cyclopropane formation, and the mechanism involves a rhodium carbenoid intermediate (Scheme 14).<sup>78</sup>

The formation of *N*-H imines and carbonyl compounds from  $\beta$ -hydroxy azides is catalyzed by cyclopentadienylruthenium dicarbonyl dimer ([CpRu(CO)<sub>2</sub>]<sub>2</sub>) under visible light. Density functional theory calculations support a mechanism involving chelation of alkoxy azide species and liberation of nitrogen leading to C–C bond cleavage.<sup>79</sup> The ring opening of two different aziridine classes with hydroperoxide provides access to  $\alpha$ - and  $\beta$ -amino and  $\alpha$ -(imino)-peroxy compounds (Scheme 15); a detailed mechanism accounting for the difference is proposed.



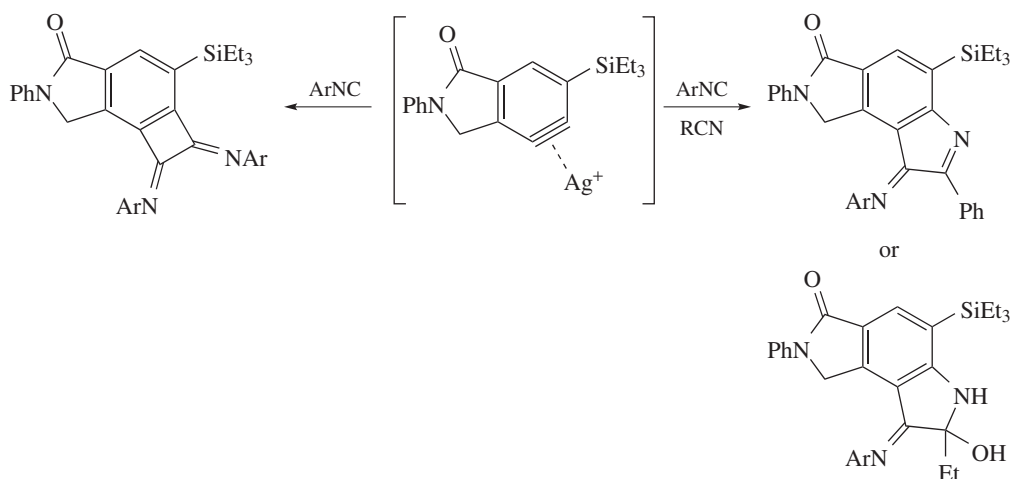
Scheme 14



Scheme 15

Further elaboration of the peroxide products gave different products under acid or base conditions.<sup>80</sup>

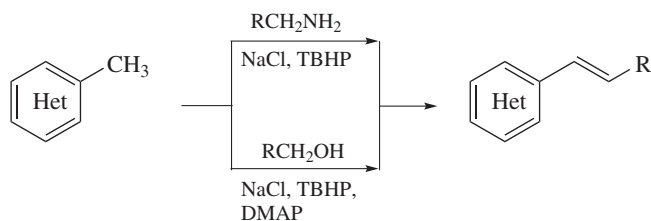
A silver-aryne complex reacts differently with isonitriles and nitriles, giving *ortho*-nitrilium organosilver arenes; interception with an isonitrile gives benzocyclobutene-1,2-diimines, while alternative reaction gives 3*H*-indol-3-imines or 3-iminoindolin-2-ols (Scheme 16).<sup>81</sup>



Scheme 16

A three-component coupling of 2-aminobenzenethiols, anilines, and methylketones leading to imino 1,4-benzothiazines using the reagent system KI/DMSO/O<sub>2</sub> has been reported. The reaction involves oxidative cyclization/coupling and proceeds with an initial oxidation of ketone  $\alpha$  C—H bond.<sup>82</sup> The aerobic oxidation of benzylamine to *N*-benzylidenebenzylamine

is catalyzed by a titanium metal–organic framework, requiring light activation.<sup>83</sup> The efficient and selective nickel-catalyzed dehydrogenation of five- and six-membered *N*-heterocycles tolerates alkyl, alkoxy, chloro, free hydroxyl and primary amine, internal and terminal olefin, trifluoromethyl, and ester functional groups; a cyclic imine intermediate is proposed.<sup>84</sup> Oxidative coupling of benzylamines or alcohols with methyl-substituted *N*-heteroarenes gives *E*-disubstituted olefins in an aqueous medium mediated by chloride (Scheme 17);  $\text{ClO}_2^-$  formed *in situ* oxidizes the benzylamine to its corresponding imine or the alcohol to its corresponding aldehyde, which in turn condenses with the arene component.<sup>85</sup>



**Scheme 17**

Highly fluorophilic ionic liquids derived from 3-iodopropyltris(3,3,4,4,5,5,6,6,7,7,8,8,8-tridecafluorooctyl)silane and *N*-alkyl imidazoles, gave imidazolium salts. These could be converted to their imidazolium salts and used to catalyze redox esterification of cinnamaldehyde with alcohols. The redox esterification was shown to proceed also in supercritical carbon dioxide, where the activity of the fluorinated catalyst was also superior to the nonfluorinated model while retaining the benefit of easy recycling.<sup>86</sup>

## Mannich and Mannich-Type Reactions

Three-component reactions of aliphatic aldehydes having one  $\alpha$ -hydrogen with *N*-methyl (benzyl)glycine and formaldehyde give Mannich bases.<sup>87</sup> Mannich base analogs of pyrrolo [3,4-*d*]pyridazinones were synthesized and shown to have better inhibitory activity against both cyclooxygenase isoforms COX1 and COX2 and a superior COX2/COX1 selectivity ratio compared to meloxicam as well as not being cytotoxic. They were also shown to reduce induced oxidative and nitrosative stress and did show binding to bovine serum albumin (BSA), suggestive of a potential long half-life *in vivo*.<sup>88</sup> The biosynthetic pathway of brevianamide A has been shown to involve the isomerase/semipinacolase BvnE that can catalyze pinacol rearrangement without a cofactor and determine the stereochemistry of the bicyclo[2.2.2]diazaoctane ring.<sup>89</sup>

The synthesis of 2-(3-arylallylidene)-3-oxindoles by the reaction of 3-diazoindolin-2-imines with 1-aryl-substituted allylic alcohols using a dirhodium(II) catalyst has been reported, and DFT calculations showed that the rate-limiting step for the formation of the desired product is the allylic C–H bond activation, leading to the elimination of TsNH<sub>2</sub>, which is favored by *p*-electron withdrawing substituents on the aryl group.<sup>90</sup> Stereoselective Mannich addition reactions using arylolefines as *C*-nucleophiles with (*S*)-*N*-*tert*-butylsulfinyl-3,3,3-trifluoroacetalimine proceed with up to 87% yield and 70:30 diastereoselectivity; this is accounted for by a reacting conformation with the bulky *t*-butyl group *anti*- to the imine double bond, in which nucleophilic attack arises from the difference in steric bulk of the sulfinyl oxygen and the oxygen electron lone pair. Deprotection gives enantiomerically pure trifluoromethylpropargylamines.<sup>91</sup>

A density functional theory study of the mechanism of the Borono–Mannich reaction using benzylamine or piperidine with pinacol allenylboronate shows that both reactions progress through coordination between the boron and the phenolic oxygen. Ring size strain and hydrogen bond activation determine the regioselectivity. In the case of benzylamine, the eight-membered ring transition structure that leads to the propargylamine product exhibits a hydrogen bond between the hydrogen attached to the nitrogen and the phenolic oxygen ( $\gamma$ -attack), whereas for piperidine, a hydrogen bond exists between the hydrogen on the imine carbon and one of the oxygens of the pinacol group in the six-membered ring transition structure toward the allenylamine ( $\alpha$ -attack).<sup>92</sup>

## Stereoselective Hydrogenation of Imines, and Other Redox Processes

It is possible to use photoimmobilized Ni clusters on a CdS photocatalyst to give imines by the dehydrogenation of amines under visible-light illumination. The process is suitable for primary and secondary amines.<sup>93</sup>

An intramolecular asymmetric reductive amination of aminoketones leading to chiral 1,4-diazepanes catalyzed by an imine reductase enzyme has been reported, which proceeds with high enantioselectivity (93% to >99%).<sup>94</sup> A review of biocatalyzed asymmetric reductive amination of carbonyl compounds and amines has appeared; it is suggested that oxidoreductases that catalyze the NAD(P)H-dependent reductive amination present advantages over amine transaminases (ATAs).<sup>95</sup> Reductive amination of glycolaldehyde leading to ethylamine products has been studied using DFT calculations that provide a rational understanding of the solvent effect in terms of energetics and kinetics. With ethylene glycol as a preferred solvent, a high yield of an unsaturated C-2-enediamine precursor can be obtained under an inert atmosphere, and its metal-catalyzed hydrogenation at elevated temperature gives *N,N,N',N'*-tetramethylethylenediamine.<sup>96</sup> A review of visible-light-driven catalytic reductive carboxylation of unsaturated hydrocarbons, organic (pseudo)halides, and imines, with CO<sub>2</sub> in the presence of mild electron donors, including amines, Hantzsch esters, and formates, has appeared.<sup>97</sup>

## Cyclizations of Imines

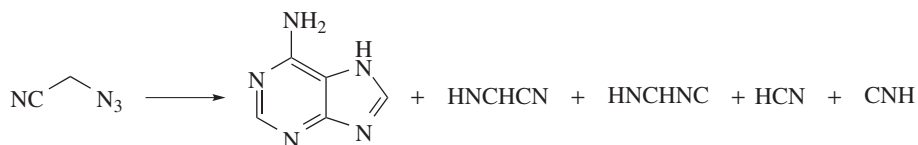
Saturated aliphatic tricycles including an imine function have been cyclized by van Leusen imidazole synthesis using *p*-toluenesulfonyl-methyl isocyanide (TosMIC). *N*-(Tosylmethyl)formamide, a decomposition product of TosMIC, was further transformed into *N*-methyleneformamide under the basic conditions and acts as a catalyst to reduce reaction times and improve yields.<sup>98</sup>

## Other Reactions of Imines

The tautomerization between an enamine and its imine is a critical step in the asymmetric Ni-catalyzed asymmetric hydrogenation of 2-oxazolones, which proceeds with 95–99% yields and 97% to >99% *ee*; 1,2-addition of a Ni(II)–H intermediate to the imine is critical.<sup>99</sup>

The photochemical and thermal decomposition of azidoacetonitrile (N<sub>3</sub>CH<sub>2</sub>CN) (Scheme 18) has been found to proceed initially by N<sub>2</sub> elimination and formation of

a closed-shell singlet nitrene, which then rapidly rearranges into formimidoyl cyanide (HNCHCN) and then formimidoyl isocyanide (HNCHNC), followed by decomposition into HCN and CNH. Under photochemical conditions, the imines and their dissociation products (HCN and CNH) form adenine.<sup>100</sup>



**Scheme 18**

The decyanation of secondary aliphatic nitriles and of malononitriles leading to alkanes in the presence of 1,3-dimethylimidazol-2-ylidene borane (diMelmd-BH<sub>3</sub>) proceeds by a radical mechanism that involves the addition of a borane radical to the nitrile to form an iminyl radical, followed by cleavage of a carbon–carbon bond. Theoretical calculations indicate that the  $\beta$ -cleavage of these iminyl radicals to give (diMelmd)BH<sub>2</sub>CN along with the corresponding alkyl radicals, is the rate-determining step in this reaction.<sup>101</sup>

MD simulations using reactive force field (ReaxFF) and density functional theory were used to investigate nitrogen transfer in the pyrolysis and hydrolysis of lignite. The nitrogen transfer in the hydrolysis system was shown to involve stepwise hydrogenation and dealkylation involving tertiary/primary amines, imines, and nitrile, including HCN as interconvertible intermediates. Hydrogen gas favored decomposition reactions of the stable tertiary amine and heterocyclic nitrogen moieties in lignite and accelerated transfer reactions of nitrogen from the solid phase into the liquid and gas phases.<sup>102</sup>

The Friedel–Crafts alkylation of 4-aminoindoles with  $\alpha$ -ketimino esters has been reported, which allows the highly regioselective formation of indole C3 and C7 alkylation products in high yields (up to 96%) and excellent enantioselectivities (up to 99% *ee*), which is catalyzed by chiral phosphoric acids. A mechanism involving hydrogen-bonding interactions of the solvent with the catalyst is proposed.<sup>103</sup>

The silver-catalyzed hydroalkoxylation of C2-alkynyl quinazolinones gives quinazolinone-fused eight-membered *N,O*-heterocycles efficiently. It appears that the silver catalyst might facilitate bidentate coordination of an imine and alkyne leading to 8-*endo-dig* cyclization to afford eight-membered *N,O*-heterocycles as well as rapid hydroalkoxylation of quinazolinones bearing terminal alkynes at the C2-position. The products significantly inhibited nitric-oxide generation in lipopolysaccharide-stimulated RAW264.7 cells, making them potential anti-inflammatory agents.<sup>104</sup>

Spirocyclic diketones with chiral all-carbon quaternary stereocenters are available by semipinacol rearrangement of vinylogous  $\alpha$ -ketols catalyzed by a cinchona-based primary amine and Brønsted acids such as *N*-Boc-phenylglycine. Quantum mechanical calculations show that the process proceeds by a sequence of nucleophilic addition, dehydration, migration, enamine–imine tautomerization, imine hydrolysis, Walden inversion, and catalyst regeneration. The cinchona-based primary amine plays a crucial role in determining the enantioselectivity, but the Brønsted acid influences the enantioselectivity much less.<sup>105</sup>

The mechanism of serine/threonine ligation has been shown to proceed through imine capture, 5-*endo-trig* cyclization, and [1,5] *O*-to-*N* acyl transfer steps, all of which occur with the assistance of pyridinium ion, using density functional theory analysis. The imine capture and 5-*endo-trig* cyclization steps are reversible, while the [1,5] *O*-to-*N* acyl transfer step is irreversible proceeding by a stepwise addition–elimination mechanism with the C–O bond cleavage as the rate-determining step.<sup>106</sup>



Annulations of *ortho*-phosphinoarenesulfonyl fluorides with trimethylsilyl azide give access to a benzo-1,2,3-thiazaphosphole in a reaction that proceeds through a Staudinger-type iminophosphorane intermediate followed by intramolecular trapping with sulfonyl fluoride.<sup>107</sup>

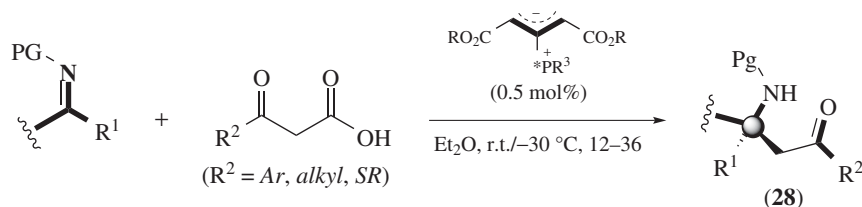
The reaction of *N*-(tosylmethyl)-substituted ureas, thioureas, and *N'*-cyanoguanidines, prepared by condensation of the corresponding amides with various aldehydes in the presence of *p*-toluenesulfinic acid and NaCN, has been studied; the outcome of the reaction is strongly dependent on the nature of the amide and the reaction conditions. Thus, *N*-(tosylmethyl)ureas give  $\alpha$ -ureido nitriles, *N*-(tosylmethyl)-*N'*-cyanoguanidines give 4-amino-2-cyanimino-1,5-dihydro-2*H*-imidazoles, and *N*-(tosylmethyl)thioureas give mixtures of imidazoles.<sup>108</sup>

3-Diazoindolin-2-imines react with nitrones to give 2-iminoindolin-3-ones under Au(I)-catalysis; the products may further react with terminal alkynes to give 2-alkynyl-2,3-dihydroquinazolin-4(1*H*)-ones under Au(I)-catalysis. A ring expansion induced by MeOH involving nucleophilic addition to a cyclic iminium intermediate is proposed.<sup>109</sup> A gold-catalyzed synthesis of 1,3-dihydrooxazolo[3,4-*a*]indoles from 1-oxo-3-yn-4-ols, nitrones, and imines has been reported; DFT calculations indicate a [3,3]-sigmatropic shift of initial alkenylgold intermediates gives an intermediate gold carbene, which then reacts with an internal alkyne.<sup>110</sup> Enantiomerically enriched amino lactones act as precursors of imino lactones, which form the corresponding azomethine ylides *in situ*, suitable for asymmetric 1,3-dipolar cycloadditions with electrophilic alkenes under silver catalysis, to give spirolactone pyrrolidines. Mechanistic details were elaborated using DFT calculations.<sup>111</sup> The 1,3-dipole annulation/allylation reaction of iminoesters and Baylis–Hillman acetates leading to fully substituted allyl imidazolidines using silver/palladium relay catalysis in high yields and regioselectivities has been reported. The mechanism involves three-component reaction initiated by silver-catalyzed 1,3-dipole annulation, followed by the sequential palladium-catalyzed allylation.<sup>112</sup> [4 + 3]-Annulations of benzopyriliums with 3-alkyl-2-diazo-3-vinyl carbonyl compounds yield 7*H*-benzo[7]annulenes under gold catalysis; the reaction is proposed to proceed by initial [4 + 2]-cycloaddition which is followed by the formation of gold carbenes, which lead to a ring expansion and migration.<sup>113</sup>

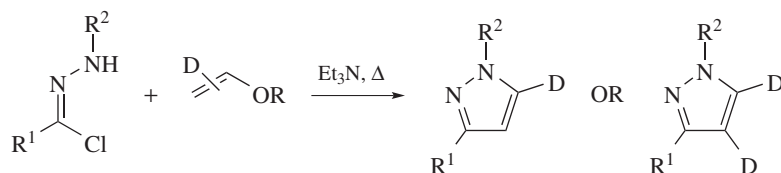
Anisylsulfanylmethylisocyanide reacts with aldehydes and ketones to afford thioimidoyl-substituted 2,5-dihydrooxazoles in the presence of BF<sub>3</sub>·OEt<sub>2</sub>. The condensation of aldehydes and ketones with 2 equiv of an isocyanide is followed by a molecular rearrangement that installs four new bonds. A similar process with imines generates *N*-substituted dihydroimidazoles. Mechanistically, BF<sub>3</sub>·OEt<sub>2</sub> activates the isocyanide to facilitate deprotonation leading to a zwitterion that traps  $\pi$ -electrophiles, and a second deprotonation–condensation with the isocyanide initiates a structural rearrangement involving a sulfanyl elimination–addition.<sup>114</sup> The [3 + 2] cycloaddition reaction between *E*-azomethine imine and 2-sulfolene was explored using molecular electron density theory at the M06-2X/6-31G(d,p) computational level. These were identified as a strong nucleophile and a moderate electrophile, respectively, and formation of the cycloadduct is irreversible, providing the driving force for the reaction. This approach allows full rationalization of both the N3-C4 regioselectivity and the *exo*-stereoselectivity. Overall, the reaction is a nonconcerted, two-stage, one-step process.<sup>115</sup>

The phosphonium-catalyzed decarboxylative condensation of cyclic ketimines and  $\beta$ -keto acids gives tertiary amine derivatives (**28**) in high yields with excellent enantioselectivities (>99% *ee*) under very low catalyst loading (0.5 mol%) (Scheme 19); a detailed mechanism is proposed in which addition of the dicarbonyl nucleophile to the imine is followed by decarboxylation.<sup>116</sup>

The reaction of vinyl ethers, as acetylene equivalents, with hydrazoneyl chlorides in the presence of triethylamine leads to 1,3-disubstituted pyrazoles, 4,5-dideuteropyrazoles and 5-deuteropyrazoles, by a mechanism involving formation of nitrile imines *in situ* followed by



Scheme 19



Scheme 20

1,3-dipolar cycloaddition to vinyl ethers to give an alkoxy pyrazoline, which by subsequent alcohol elimination gives the product (Scheme 20).<sup>117</sup>

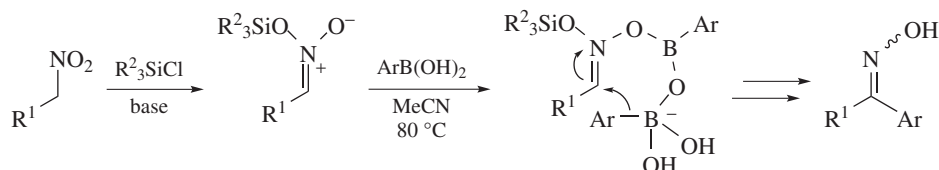
ee

## Oximes, Oxime Ethers, and Oxime Esters

Reviews of the radical-mediated non-photocatalyzed and photocatalyzed cross-coupling of cycloketone oximes,<sup>118</sup> and of the application of iminoxyl radicals in synthesis along with their generation, structure, stability, and spectral properties, have appeared.<sup>119</sup> Cascade cyclizations of unsaturated oxime esters or ethers have been reviewed.<sup>120</sup> Reviews of methodologies for the synthesis of isoxazolines, classified into iminoxyl radical-initiated intramolecular cyclization, intermolecular radical addition-initiated cyclization, intramolecular nucleophilic cyclization, [3 + 2] cycloaddition, and [2 + 2 + 1] cycloaddition,<sup>121</sup> and of the synthesis of isoxazoles and their derivatives, prepared by metal catalyzed or mediated cyclization/functionalization of alkynone oxime ethers, acetylenic oximes, propargylic amino ethers, alkynyl nitrile oxides, and propargylic alcohols have appeared.<sup>122</sup> Oximes have been found to mediate the visible-light photoredox-catalyzed regioselective sulfonylation of alkenes with sulfonyl hydrazides at room temperature; the hydroxyl group of the oxime appears to be crucial for the success of this process.<sup>123</sup> The phosphoranyl radical-mediated deoxygenative functionalizations of alcohols, carboxylic acids, oximes, and sulfoxides with a particular emphasis on reaction scope and mechanism have been reviewed.<sup>124</sup>

The metal-free addition of boronic acids to silylnitronates gives oximes; a reaction mechanism involving a seven-membered ring transition state leading to aryl migration (Scheme 21).<sup>125</sup>

The silver-catalyzed radical ring-opening cyclopropanols with sulfonyl oxime ethers give  $\gamma$ -keto oxime ethers with moderate to good yields, in a stereoselective manner for



Scheme 21